

USING MATLAB TO CREATE AN IMAGE FROM RADAR

Douglas Hulbert
Mathematics Department
Norfolk State University
700 Park Avenue Unit 2483
Norfolk VA 23504-8060
dhulbert@nsu.edu

Introduction. Digital imaging algorithms developed over the last thirty years have made remarkable progress in our ability to make accurate images of planets, ocean floors, and the interiors of living organisms. Algorithms used in synthetic aperture radar (SAR) have many similarities with those used in x-ray computerized axial tomography (CAT), magnetic resonance imaging (MRI), ultrasound and acoustic imaging, and radio astronomy. While these disciplines have evolved in many complex ways, several key aspects of digital image processing can be understood using concepts from a standard undergraduate mathematics curriculum.

Outline. The purpose of this paper is twofold:

- to describe the radar imaging process using concepts from undergraduate mathematics courses
- to present images generated by the mathematical software in MATLAB® to give examples of a few of these concepts.

D equals r times t. The concept of *echo-ranging* states that, in a medium of known propagation speed, the round-trip flight time of a signal, multiplied by the signal propagation speed, is equal to twice the range from the signal source to the signal reflector. If c denotes the speed of propagation, the range to the reflector is

$$r = \frac{ct}{2}$$

The simplest problem: estimating reflectivity of a discrete set of reflectors of known sizes and distinct ranges. Because the reflectors have distinct ranges, their reflectivities can be estimated by measuring returned signal strength at distinct arrival times; then reflectivities vary directly with received amplitudes and inversely with cross-sectional area. If two reflectors were to have identical ranges, their echoes would be combined in some unknown way, and the respective reflectivities could not be estimated.

The problem of closely spaced reflectors. Echo ranging works well when reflectors are isolated from one another, as when a radar is looking upward and the reflectors are isolated aircraft. When an airborne radar is looking downward, echo ranging doesn't work very well because ground returns arrive in a continuous stream. Furthermore, there is an inherent conflict (even with a discrete set of reflectors) between the radar's ability to resolve range and its ability to detect weak echoes. The reason is: shorter pulses enable

the discrimination of more closely spaced reflectors, while longer pulses allow the radar to integrate reflected energy over a longer period and thereby distinguish between reflected signal energy and interfering energy sources such as thermal noise. That is, longer pulses tend to increase the signal-to-noise ratio, or SNR. Figure 1 depicts the problem of overlapping returns when range differences between successive reflectors become shorter than the duration of the illuminating transmit pulse. Notice that the duration of each echo is equal to the duration of the transmitted pulse.

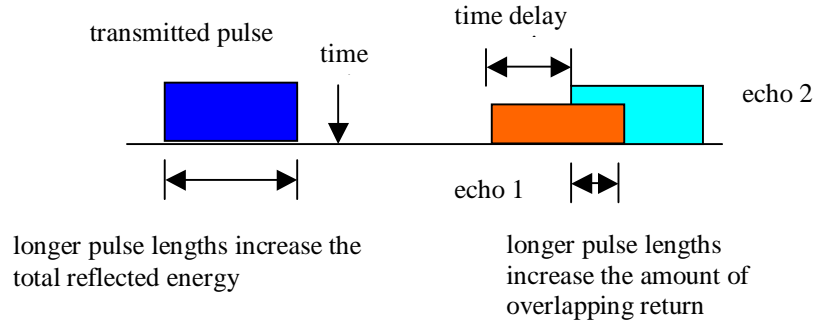


Figure 1 Range resolution vs. total illumination energy

The term **pulse compression** denotes various methods of encoding the phase of the transmitted signal to effectively shorten the length of the transmit pulse. In a *chirp* waveform, for example, the transmitted energy sweeps through a wide range of frequencies, allowing the radar receiver to listen while the transmitter is active (transmitting and receiving at the same frequency simultaneously and in the same proximity can destroy sensitive circuitry). The duration of a frequency-modulated (FM) chirp can be on the order of 500 times the effective duration of simple pulse processing scheme having the same range resolution. The chirp **transmitted waveform** can be written as

$$p(t) = a(t) \exp(i\beta t + i\alpha t^2) \quad (1)$$

where $a(t)$ represents a real-valued, positive function called the signal envelope or windowing function. The **echo** from reflectors with reflected energies x_k at ranges r_k is represented by a sum of delayed signals

$$s(t) = \sum_k x_k a(t - 2r_k / c) \exp(i\beta(t - 2r_k / c) + i\alpha(t - 2r_k / c)^2) \quad (2)$$

Processing the echo. In engineering terms, the return signal is mixed with delayed in-phase and quadrature versions of the transmitted FM chirp and low-pass filtered. In mathematical terms, the received signal $s(t)$ is multiplied by the complex conjugate of a replica of the transmitted signal $p(t)$ to obtain

$$s(t)p^*(t) = \sum_k x_k a(t - t_k) \exp(-i\beta t_k + i\alpha t_k^2) \exp(-i\alpha t_k t), \quad (3)$$

where $t_k = 2r_k/c$. Next the signal (3) is passed through an analog-to-digital converter to collect samples for digital processing. Using j as a sampling index for discrete t -values, (3) becomes

$$s(t_j)p^*(t_j) = \sum_k x_k a(t_j - t_k) \exp(-i\beta t_k + i\alpha t_k^2) \exp(-i\alpha t_k t_j) \quad (4)$$

If there are m samples taken of the received waveform, and n unknown reflected energies, then (4) constitutes a set of m linear equations in n unknowns, i.e.,

$$\sum_{k=1}^n A_{j,k} x_k = b_j, j=1, \dots, m \quad \text{or} \quad \mathbf{Ax} = \mathbf{b} \quad (5a)$$

where

$$A_{j,k} = a(t_j - t_k) \exp(-i\beta t_k + i\alpha t_k^2) \exp(-i\alpha t_k t_j) \quad \text{for } j=1, \dots, m \text{ and } k=1, \dots, n \quad (5b)$$

and

$$b_j = s(t_j)p^*(t_j) \quad \text{for } j=1, \dots, m \quad (5c)$$

When the t_j and t_k are uniformly spaced and the coefficient matrix is approximated by the complex exponentials $\exp(-i\alpha t_k t_j)$, the mapping represented by A in (5a) is called the *discrete Fourier transform* (DFT). When A represents a DFT, it is unitary so that its inverse is the transpose of its complex conjugate.

The model embodied in (5) is only an approximation, so that the solutions $\{x_k\}$ have limitations even though (5) is numerically well-posed. The reason is that, in the limiting case of a continuous ground reflectivity function and an infinitesimal sampling interval, the finite duration of the chirp waveform (the finite support of a^*) causes the true values of the reflectivity function to be distributed among the solutions $\{x_j\}$ by means of a convolution called the *point spread function* (psf). For example, if the envelope a^* is a simple step function with range $\{0,1\}$, then the psf is of the form $\sin(u)/u$. As the duration of the chirp waveform increases, the support of the psf narrows and the accuracy of the solutions $\{x_j\}$ increases.

Cross-range resolution: the two-dimensional Fourier transform. The next step in our development is to leap another dimension further into a multiplicity of data collection and record the returns from a number of chirped waveforms. Our model for this larger interval of collection includes the following assumptions.

- Each chirp collection interval is modeled as a time during which the radar platform is stationary (the platform moves, but displacement is negligible)

- Between chirp collection intervals the radar platform moves but its antenna turns with respect to the line of platform motion (slews) in a way that keeps its line-of-sight coincident with a fixed point on the ground called the *scene center*
- The reference point for the range measure set $\{t_k\}$ or $\{2r_k/c\}$ of Equations (2)-(5) is changed from one chirp collection interval to the next so that the time delays / spatial offsets are always referred to the scene center.
- The range from the radar platform to the scene center is large enough so that spheres of constant range are treated as straight lines where they intersect the ground.

Figure 2 below depicts these assumptions. With the notation introduced in Figure 3 we will rewrite (3), bringing it into the form of a double integral. We first make the following substitutions in (3):

- $t_k = 2r_k/c$
- $x_k = f(x_k, y_k)\Delta_k$, where $f(x, y)$ is unknown reflectivity and Δ_k is reflector area
- $a(t - t_k) = 1$ inside the scene of interest
- $\exp(-i\beta t_k + i\alpha t_k^2) = 1$ as it is compensated by hardware pre-processing
- $r_k = x_k \cos \theta + y_k \sin \theta$, where θ is the angle that the radar line of sight makes with the scene reference axis (Figure 3).

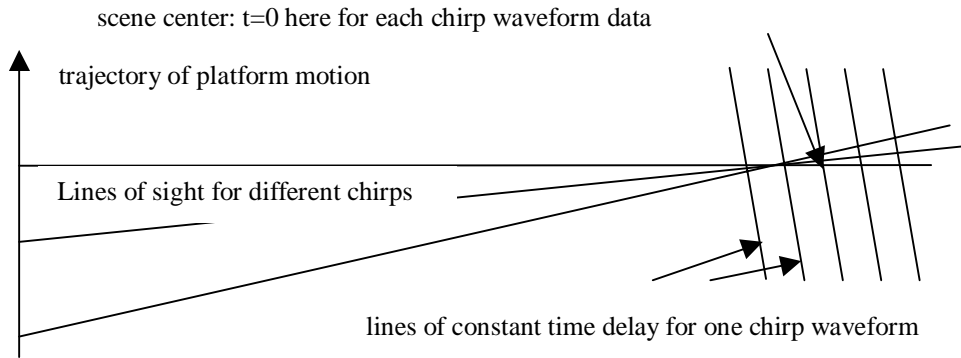


Figure 2: Platform positions, lines of sight, and scene center

Combining these we obtain

$$s(t)p^*(t) = \sum_k f(x_k, y_k)\Delta_k \exp\left[-i\frac{2\alpha t}{c}(x_k \cos \theta + y_k \sin \theta)\right] \quad (6)$$

Next, we assume that the reflector surfaces form a partition of the scene of interest, so that (6) can be understood as a double integral. In particular, the new form is of a Fourier transform in two dimensions:

$$s(t)p^*(t) = \iint_{scene} f(x, y) \exp[-i(xX + yY)] dx dy, \quad (7a)$$

where

$$(X, Y) = \left(\frac{2\alpha t}{c} \cos \theta, \frac{2\alpha t}{c} \sin \theta \right) \quad (7b)$$

is a measure of *spatial frequency* with units in each dimension of cycles per unit length. In (7b), as the returns of one chirp waveform are processed, the variable t runs through a representative discrete set of values as indexed by j in (5a,b,c). As the radar platform moves along its trajectory (Figure 2), the variable θ (Figure 3) runs through a discrete set of values called the collection *aperture*. In the (X, Y) spatial frequency domain, this discrete set of points takes on the appearance of seats in an amphitheater (Figure 4).

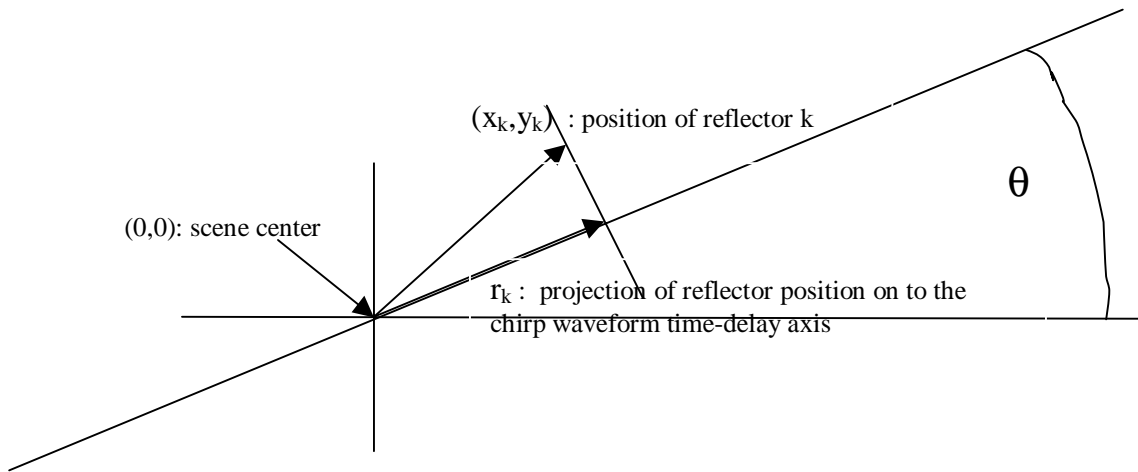


Figure 3: Positions in scene coordinates and projections onto one time-delay axis

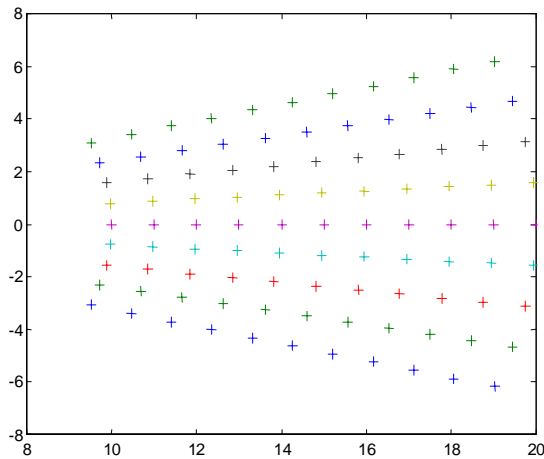


Figure 4 Location of data collection points in spatial frequency coordinates

The determination of the reflectivity $f(x,y)$ is then based its correspondence with a Fourier dual $F(X,Y)$. The two functions are paired via the two-dimensional Fourier transform as

$$F(X,Y) = \int_{-\infty}^{\infty} \int_{-\infty}^{\infty} f(x,y)e^{-i(xX+yY)} dx dy \quad \text{and} \quad f(x,y) = \int_{-\infty}^{\infty} \int_{-\infty}^{\infty} F(X,Y)e^{i(xX+yY)} dx dy \quad (8a,b)$$

From (7) and (8) we have

$$F(X,Y) = F\left(\frac{2\alpha t}{c} \cos \theta, \frac{2\alpha t}{c} \sin \theta\right) \quad (9)$$

The *polar reformatting algorithm* is a commonly used method of recapturing $f(x,y)$ from $F(X,Y)$, in which values of F , with collection points depicted in Figure 4, are interpolated to a rectangular grid in (X,Y) space, and thence to a rectangular grid in (x,y) space. The rectangular grid in the spatial frequency domain is chosen as a way station for the information because of the existence of a very fast transform from the rectangular (X,Y) grid to the spatial (x,y) domain known as the *Fast Fourier Transform*, or *FFT*.

MATLAB images for a single point reflector. We conclude with a pair of MATLAB images which depict an idealized set of radar returns from a single reflector at scene center. Figure 5 depicts data on input from the receiver, Figure 6 at output to a screen. . For both figures, the matrix of amplitudes is 512-by-512.

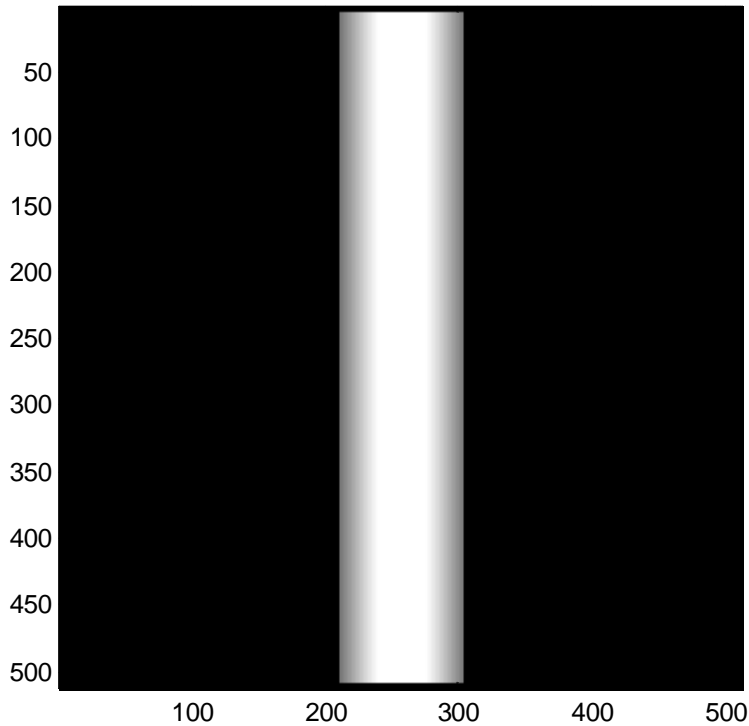


Figure 5: Amplitude of collected data pairs (I,Q) for a point reflector

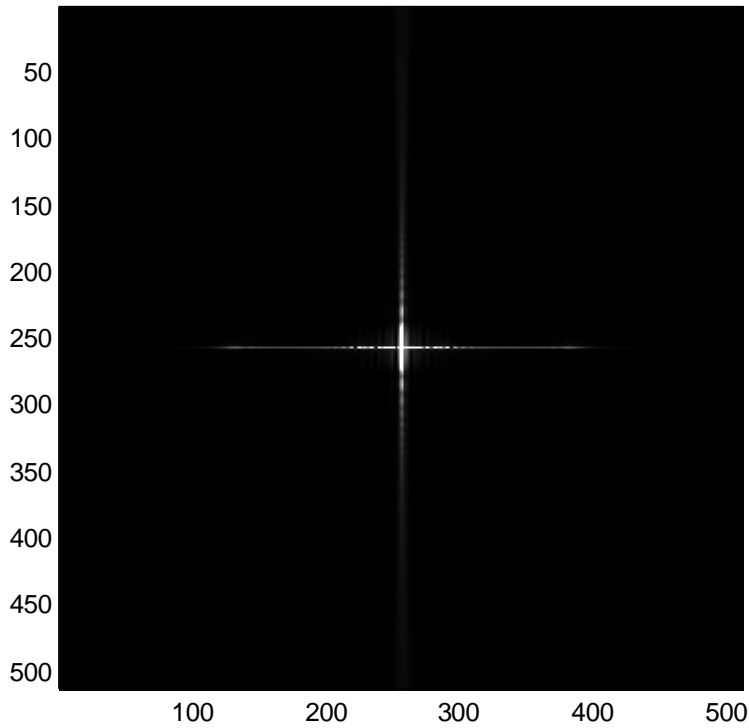


Figure 6: Image of the point reflector

Figure 5 portrays amplitudes of collected complex-valued returns from the radar receiver: lighter color indicates greater amplitude. The horizontal axis is indexed by j in (4), i.e., the time index within a chirp collection interval. Within each row of pixels, this time is referred to the time that the midpoint of a chirp waveform returns from the scene center; it is called "fast time." The vertical axis in Figure 5 counts successive chirp waveforms, i.e., successive values of θ in (6) and (7). This count of look angle (or waveform processing interval or aperture index) is called "slow time."

Figure 6 gives the final image of the point reflector, i.e., the reflectivity function $f(x,y)$ in geographic coordinates, range along the horizontal axis, cross-range (distance along the platform trajectory) along the vertical. The smearing along the horizontal is caused by a point spread function as discussed above. The smearing along the vertical is caused by a similar point spread effect, influenced by the number of cross-range data collection points.

References

Jackowatz, C.V., D.E. Wahl, P.H. Eichel, D.C. Ghiglia, P.T. Thompson, *Spotlight Mode Synthetic Aperture Radar: a Signal-Processing Approach*, Kluwer Academic, Boston, 1996

Soumekh, Mehrdad, *Synthetic Aperture Radar Signal Processing with MATLAB Algorithms*, John Wiley and Sons, New York, 1999